Mathl. Comput. Modelling Vol. 16, No. 3, pp. 109–120, 1992
Printed in Great Britain.

0895-7177/92 $5.00 + 0.00

MODELING PHASE VOLUME CONSTRAINTS UNDER REPETITIVE DECOMPRESSION

B. R. WIENKE
Applied Theoretical Physics Division
Los Alamos National Laboratory
Los Alamos, NM 87545, U.S.A.

(Received September 1991)

Abstract—Extending the critical volume (separated phase) hypothesis in time integral form to repetitive decompressions, we show that reduced gradients following repetitive exposures are necessary in time, in any model, to maintain the separated nitrogen in tissue (bubbles) below a limit point. A realistic bubble model is then discussed, systematized, and applied to some marginal decompression profiles. The focus is permissible bubble excess, not dissolved gas *per se*, though reductions affect all compartments, fast and slow, requiring a systematic lowering of repetitive tensions. Deep repetitive and shallower multi-day exposures are impacted by the procedure. Within nucleation theory, deeper-than-first exposures are also treated. A set of exposure fractions, ξ, accounting for micronuclei excitation and regeneration, reduced bubble elimination in repetitive activity and coupled effects on tissue tension is discussed, with ξ representing a set of multiplicative factors (less than one) reducing critical parameters controlling exposures. These factors penalize repetitive activity between short time spans, deeper-than-previous and continuous multi-day activities, compared to standard algorithms using a fixed slow compartment. Within the approach, fast compartments, controlling deeper exposures, are impacted the most, but slow compartments are also affected.

INTRODUCTION

Haldane decompression models [1–17] address just dissolved tissue gas, and therefore, the longer the bulk of tissue gas remains in the dissolved state, the more correct and useful will prove such an approach. But as increasing proportions of free phases [18–25] grow, by direct excitation of critical micronuclei or bubble coalescing transitions, that classical algorithm loses some predictive basis in using a dissolved gas buildup to limit exposures. The critical phase model limits free gas buildup, alternatively coupling dissolved and free phases, is realistic, and forms the basis of this analysis of repetitive decompression. The end result of imposing a separated phases constraint is a reduction in permissible free-dissolved gas gradients or, equivalently, tissue tensions in repetitive exposures.

Bubbles and dissolved gas are considered within the critical phase hypothesis [19]. A repetitive criterion is developed, underscoring the reduction in critical parameters, and its application to marginal profiles is discussed. The reduction arises from lessened degree of bubble elimination over repetitive intervals, compared to long bounce intervals, and the need to reduce bubble inflation rate through smaller driving gradients. Deep repetitive and spike exposures feel the greatest effects of gradient reduction, but shallower multi-day activities are impacted. Development and application is bubble model specific for illustration, yet implications of the phase volume constraint are more general. Bounce decompressions enjoy long surface intervals to eliminate bubbles within the critical phase hypothesis, while repetitive decompressions must contend with shorter intervals, and thus, a reduced time for bubble elimination. Theoretically, a reduction in the bubble inflation driving term, namely, the tissue gradient or tension, holds the inflation rate down. The concern is the bubble excess driven by dissolved gas.

We thank colleagues and friends for their help and advice in this analysis, especially Tom Kunkle (LANL), David Yount (University of Hawaii), Doug Toth and Richard Bonin (SCUBAPRO Industries) and Steven Shankle (INSIGHT Incorporated). Thanks to the Los Alamos National Laboratory (LANL) for personal support.

Consistent with the phase constraint three reduction factors, addressing bubble regeneration, deeper-than-previous excitation of nuclei and shorter repetitive time spans for excess bubble elimination, are defined and applied to some marginal exposures, namely, two repetitive dives to 120 fsw for 10 min with a 2 hour surface interval, repeated for three days. Three repetitive dives to 120 fsw for 10 min with 2 hour surface intervals, on one day, is known to cause bends in roughly three out of four cases, according to Leitch and Barnard [25], so the exercise is not academic.

GAS DYNAMICS

The inert gas exchange is driven by the local gradient, the difference between the arterial blood tension, p_a, and the instantaneous tissue tension, p. Such behavior is modeled in time, t, by mathematical classes of *exponential* response functions, bounded by p_a and the initial value of p, denoted p_i. These multi-tissue functions are well known, tracking both dissolved gas buildup and elimination symmetrically,

$$p = p_a + (p_i - p_a) \exp(-\lambda t), \tag{1}$$

with the perfusion constant, λ, related to the tissue half-time τ, through the usual,

$$\lambda = \frac{0.6931}{\tau}. \tag{2}$$

Compartments with 1, 2, 5, 10, 20, 40, 80, 120, 180, 240, 360, 480 and 720 min half-lives, τ, are a realistic spectrum, according to inert gas washout experiments, and are independent of pressure. The tensions, p_i and p_a, represent extremes for each stage, or more precisely, the initial tension and the arterial tension at the beginning of the next stage. Classical models limit exposures by requiring that the tissue tensions never exceed the critical tensions, fitted [20] to the US Navy non-stop limits, for example, in units of absolute pressure (fsw), by

$$M = 193.3\,\tau^{-1/4} + 4.110\,d\,\tau^{-1/4}. \tag{3}$$

Such a fit, with a $\tau^{-1/4}$ dependence, is generic to present critical tensions, and the corresponding critical gradient, G, is given by (with P, ambient pressure)

$$G = M - P. \tag{4}$$

Bubbles, which are unstable, might grow from stable, micron size, gas nuclei which resist collapse, due to elastic skins [23] of surface-activated molecules (surfactants), or possibly reduction in surface tension [16] at tissue interfaces. If families of these micronuclei persist, they vary in size, surfactant content, tissue location, effective surface tension on excitation to growth and number density. Large pressures (somewhere near 10 atm) are necessary to crush them. Micronuclei are small enough to pass through the pulmonary filters, yet dense enough not to float to the surfaces of their environments, with which they are in both hydrostatic (pressure) and diffusion (gas flow) equilibrium. Compression-decompression is thought to excite them into growth. Ordinarily, the bubble skins are permeable to gas, but can become impermeable when subjected to hefty compressions (again 10 atm), outside nominal activity.

A model of skin behavior, called the varying-permeability model (VPM), was proposed by Yount [23] and Strauss [18], and extended by Kunkle [7] and other co-workers [21–25]. Rudimentary discussions of nucleation and decompression can be traced to Walder [14]. By tracking changes in nuclear radius that are caused by increasing or decreasing pressure, the VPM has correlated quantitative descriptions of bubble-counting experiments carried out in a supersaturated gel [22,24]. The model has also been used to trace levels of incidence of DCS in animal species such as shrimp, salmon, rats and humans. Microscopic evidence has been gathered, suggesting spherical gas nuclei do exist and possess physical properties consistent with earlier assignments. For example, the nuclear radii are on the order of 1 micron or less, and their number density in bio-media decreases exponentially with the increasing of radius, a characteristic of systems

Table 1. Exposure fractions (120/10, 0/120, 120/10 for three days).

τ (min)	ΔG (fsw μm)	G_0 (fsw)	ξ_1	ξ_2	ξ_3	ξ_4	ξ_5	ξ_6
1	82.0	192.4	1.00	.95	.93	.88	.86	.80
2	81.6	150.0	1.00	.95	.93	.88	.86	.81
5	81.3	93.9	1.00	.95	.93	.88	.86	.81
10	80.7	64.9	1.00	.95	.93	.89	.86	.82
20	79.9	45.6	1.00	.95	.93	.89	.86	.82
40	73.8	33.8	1.00	.96	.93	.89	.86	.82
80	65.9	25.9	1.00	.96	.93	.89	.86	.82
120	59.8	22.2	1.00	.96	.93	.90	.86	.82
180	55.9	18.1	1.00	.97	.93	.90	.86	.83
240	51.9	15.5	1.00	.97	.93	.90	.86	.84
360	50.5	12.1	1.00	.98	.93	.91	.86	.84
480	49.5	10.5	1.00	.98	.93	.91	.86	.85
720	47.8	8.3	1.00	1.00	.93	.93	.86	.86

of VPM nuclei in equilibrium with their surroundings at the same temperature [23]. Preformed nuclei have also been seen in serum and egg albumin.

A critical radius, r_0, at a fixed pressure P_0, represents a cutoff for growth upon a decompression to lesser pressure. Nuclei larger than r_0 potentially grow upon decompression. Additionally, following an initial compression to some $P > P_0$, a smaller class of micronuclei with critical radius, r, can be excited into growth with decompression. If r_0 is the critical radius at P_0, then, according to Yount and Hoffman [21], the smaller family, r, exited by decompression from a pressure P, obeys,

$$\frac{1}{r} = \frac{1}{r_0} + \frac{\Delta P}{158}, \tag{5}$$

with $\Delta P = P - P_0$ measured in fsw and r in microns. Deeper decompressions excite smaller, more stable, nuclei than shallower decompressions.

Since the tissue deformation and impairment of circulation should depend on both the size and number of bubbles, it seems plausible that the total volume of evolved gas would serve as an effective criteria in any bubble model, with the bubble numbers fluctuating accordingly [21]. For shorter decompression times, bubble nuclei have little time to inflate. The permissible critical radius is then smaller, and the allowed supersaturation larger, resulting in many small bubbles. Conversely, during long decompressions, bubbles may grow very large, so that only a few are permitted.

CRITICAL GRADIENTS AND NUCLEI

Any set of non-stop time limits can be plugged into (1), ensuing maximum tensions across all compartments and depths assigned at the critical tensions. The corresponding critical supersaturation gradients, G, are obtained by subtracting off the ambient pressures, P, as seen in (4). Using a set of reduced time limits, t_{nd}, limited by $dt_{nd}^{1/2} = 380$ fsw min at the bounce depth d, it is easy to construct a conservative set of gradients for purposes of discussion. The critical gradient, G, is written for each compartment τ, using the non-stop limits, and the excitation inverse radial difference Δr^{-1}, from (5),

$$G = \Delta r^{-1}\Delta G + G_0, \qquad \Delta r^{-1} = \frac{1}{r} - \frac{1}{r_0}, \tag{6}$$

at depth $d = P - 33$ fsw. A non-stop exposure, followed by direct return to the surface, thus allows G_0 for that compartment. Both G_0 and ΔG are tabulated in Table 1, with ΔG extracted from [2]. The gradient change, ΔG, affects decompression exposures. Because the time limits are conservative, the supersaturation gradients are also conservative. Figure 1 plots G as a function of r for the 2, 10, 40, 120 and 720 min tissues.

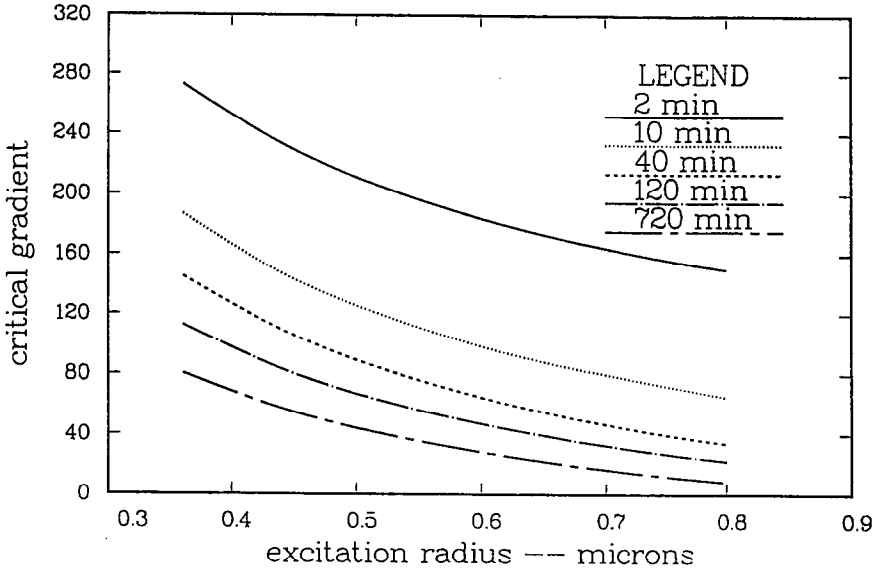

Figure 1. Critical gradients.

The minimum excitation, G^{bub}, initially probing $r(t)$ and accounting for regeneration [21] of nuclei over time scales τ_d, is

$$G^{bub} = \frac{2\gamma\,(\gamma_c - \gamma)}{\gamma_c\, r(t)} = \frac{11.01}{r(t)} \quad \text{(fsw)}, \tag{7}$$

with

$$r(t) = r + (r_0 - r)\,[1 - \exp\,(-\omega t)], \tag{8}$$

γ, γ_c, the film, surfactant surface tensions, that is, $\gamma = 17.9$ dyne/cm, $\gamma_c = 257$ dyne/cm, and ω the inverse of the regeneration time for stabilized gas micronuclei (many days). The critical radii of the nuclei probed depend on the depth according to (5). The excitation threshold, G^{bub}, represents that minimal free-dissolved gas gradient, just balanced by the surface tension, supporting growth. Prolonged exposure leads to saturation, and the largest possible gradient, G^{sat}, can be equivalenced to the Hills [16], Hennessy and Hempleman [19] and Yount and Hoffman [21] parameterization

$$G^{sat} = 58.6\,\Delta r^{-1} + 23.3 = 0.372\,P + 11.01 \quad \text{(fsw)}. \tag{9}$$

The relationship for G^{sat}, deduced from the exposure data and given by (9), agrees with the specific parameterization of the controlling compartment in critical tension algorithms. That is, the critical tensions extracted from the non-stop limits for one slow compartment, τ^{sat}, with $120 \leq \tau^{sat} \leq 720$ min (generally), are used to limit extended exposures.

At the surface, $G^{bub} = 13.8$ fsw, while $G^{sat} = 23.3$ fsw. At 240 fsw, $G^{bub} = 30.4$ fsw, and $G^{sat} = 100.3$ fsw. What is seen here is a reflection of the body's ability to maintain higher degrees of supersaturation with increased pressure. Bubbles and micronuclei tend to both shrink and stabilize under pressure, permitting increased levels of supersaturation because of greater surface tension pressure ($2\gamma/r$). Under decompression, smaller bubbles and nuclei also grow more slowly for the same reason. The surface tension pressure, varying inversely as the spherical radius r, helps to expel gas in the pocket, by squeezing and building up a diffusion gradient across the film boundary. Unless the nuclei are stabilized so that the net surface tension pressure is zero, all nuclei would eventually collapse upon themselves because of this squeeze. When the nuclei are squeezed by an increasing pressure, the experiments established that they stabilize at new smaller radius, not growing back to earlier sizes unless the ambient pressure is reduced [24].

From (7), it is clear that the effective surface tension, G^{bub}, varies inversely as $r(t)$. The corresponding critical tensions and gradients, then, also vary as G^{bub} in the VPM. Consistently

with (6)–(8), we write

$$M(t) = M - \frac{2\gamma(\gamma_c - \gamma)}{\gamma_c}\left(\frac{1}{r} - \frac{1}{r(t)}\right), \tag{10}$$

with r, the excitation radius for an appropriate bounce decompression. As $t \to \infty$, $M(t)$ is decreased by the difference of the inverse asymptotic excitation radii. If $r(t)$ grows as $t \to \infty$, critical tensions in fast tissues will be reduced more than in slow tissues. If $r(t)$ shrinks as $t \to \infty$, the opposite is true. In terms of just regeneration phase parameters, we have

$$M(t) = M - \frac{11.01}{r(t)}\frac{(r - r_0)}{r}[1 - \exp(-\omega t)]. \tag{11}$$

Such a critical tension accounts only for regeneration, but can be more generally expanded for repetitive decompressions in the extended phase volume scheme.

Although the actual size distribution of gas nuclei in humans is unknown, experiments [24,25] *in vitro* suggest that a decaying exponential is reasonable,

$$n = N\exp(-\beta r), \tag{12}$$

with β a VPM constant and N a convenient normalization factor across the distribution. For small values of the argument, βr,

$$\exp(-\beta r) \approx 1 - \beta r, \tag{13}$$

as a linear simplification. For a stabilized distribution, n_0, accommodated by the body at a fixed pressure P_0, the excess number of nuclei, Δn, excited by compression-decompression from a new pressure P, is, with (5) tracking the change in radius r,

$$\Delta n = n_0 - n \approx N\beta r_0\left(1 - \frac{r}{r_0}\right) = N\beta r_0 \Delta r^{-1}. \tag{14}$$

For deep compressions-decompressions, Δn is large, while for shallow compressions-decompressions, Δn is small. When Δn is folded over the gradient G, in time, the product serves as a critical volume indicator and can be used as a exposure limit point in the following way.

CRITICAL VOLUME HYPOTHESIS

The rate at which gas inflates in a tissue depends upon both the excess bubble number, Δn, and the supersaturation gradient, G. The critical volume hypothesis requires that the integral of the product of the two must always remain less than some limit point, αV^{crit}, with α a proportionality constant. Accordingly, this requires (see [21])

$$\int_0^\infty \Delta n\ G\ dt = \alpha V^{\text{crit}}, \tag{15}$$

for V^{crit} the limiting gas volume. Assuming that the tissue gas gradients are constant during the ascent time t_d, while decaying exponentially to zero afterwards, and taking the limiting condition of the equal sign, yields for a bounce decompression,

$$\Delta n\ G\ (t_d + \lambda^{-1}) = \alpha V^{\text{crit}}. \tag{16}$$

For non-stop exposures with linear ascent rate ν , we have $t_d = d/\nu$. With saturation exposures, the integral must be evaluated iteratively over the component decompression stages, maximizing each G while satisfying (15). In the latter case, t_d is the sum of individual stage times plus interstage ascent times, assuming the same interstage ascent speed, ν.

Implicit in the integral approach is the assumption that free gas is continuously leaving the body. The excess, Δn, then represents the difference between the actual bubble number and the amount safely eliminated by the body. The excess bubble number is only regulated through each step of a single exposure, so that in evaluating the integral over time, the assumption is

made that the bubble number, Δn, depends on the initial and final pressures (that is, surface, P_0, compression to P, and then decompression back to P_0) typical of bounce or saturation (slow bleed) exposures. Employing Equation (15) iteratively, and one more constant, δ, defined by

$$\delta = \frac{\gamma_c \alpha V^{\text{crit}}}{\gamma \beta r_0 N} = 7500 \text{ fsw min}, \tag{17}$$

Equation (16) is recast, using (14),

$$\left(1 - \frac{r}{r_0}\right) G(t_d + \lambda^{-1}) = \delta \frac{\gamma}{\gamma_c} = 522.3 \text{ fsw min} \tag{18}$$

according to Yount and Hoffman [21], who correlated data for bounce and saturation exposures. Repetitive exposures were not, however, included in the analysis. Their non-stop limits are very close to ours, while the corresponding gradients are slightly larger than ours, because the non-stop limits are slightly greater. Succinctly phrased, our δ, is less than 7500 fsw min, nearer 7300 fsw min. If the US Navy bounce limits are similarly bootstrapped with (16), a value of δ around 7900 fsw min is deduced. Clearly, any set of non-stop time limits agreeable to a table designer could be plugged into (15)–(18), and a set of bootstrapped critical bounce gradients and tensions generated, with a set of model parameters, γ, γ_c, δ, ω and r_0.

The parameters γ, γ_c, δ, ω and r_0 are five of the fundamental constants in the model. In terms of (5) and the depth at which a compartment controls the exposure, according to Figure 1, the radii of nuclei excited as a function of controlling half-life, τ, in the range, $12 \leq d \leq 220$ fsw, are fitted by

$$1 - \Delta r^{-1} = \frac{r}{r_0} = 0.9 - 0.43 \exp(-0.0559\, \tau), \tag{19}$$

with the half-life τ, measured in minutes. For a large τ, r is close to r_0, while for small τ, r is on the order of $0.5 r_0$. For multi-exposures, another time scale parameter, χ, mainly affecting repetitive intervals, is required. The time scales for χ^{-1} are in the hour range, considering the bubble growth experiments [7,18], which contrast with time scale for regeneration, ω^{-1}, on the order of many days.

EXTENDED CRITICAL VOLUME HYPOTHESIS

In extending the model to repetitive exposures, as a simple starting point we assume that the bubble excess is roughly constant over multi-exposures, perhaps a liberal assumption, but then counter with worse case conditions in neglecting any phase volume reductions over surface intervals, a conservative assumption. In some sense, they are offsetting assumptions. Larger excesses ultimately spawn larger phase volumes, but some phase volume reduction over surface intervals allows larger excesses. This is a point we are investigating, and hope to report later.

Here, we extend the critical phase criterion to repetitive decompressions, that is, the integral of (15) to multi-exposures, by writing

$$\sum_{j=1}^{J} \left[\Delta n\, G\, t_{d_j} + \int_0^{t_j} \Delta n\, G\, dt\right] \leq \alpha V^{\text{crit}}, \tag{20}$$

with the index j denoting each segment, up to a total of J, and t_j the surface interval after j^{th} segment. The particular G are general, and not necessarily the set derived for bounce and saturation exposures. However, it is useful to extract G from the standard set for meter convenience and computational simplicity, effectively generating constraints on multi-exposures, as function of time and depth, and controlling half-life.

For the inequality to hold, that is, for the sum of all growth rate terms in (20) to total less than αV^{crit}, obviously each term must be less the αV_{crit}. Performing the indicated operations and assuming $t_J \to \infty$, gives

$$\sum_{j=1}^{J-1} \left[\Delta n\, G\left[t_{d_j} + \lambda^{-1} - \lambda^{-1} \exp(-\lambda t_j)\right]\right] + \Delta n\, G(t_{d_j} + \lambda^{-1}) \leq \alpha V^{\text{crit}}. \tag{21}$$

Defining G_j:

$$\Delta n\, G_j\,(t_{d_j} + \lambda^{-1}) = \Delta n\, G\,(t_{d_j} + \lambda^{-1}) - \Delta n\, G\, \lambda^{-1} \exp\,(-\lambda\, t_{j-1}), \qquad \text{for } 2, \ldots, J, \tag{22}$$

and

$$\Delta n\, G_1 = \Delta n\, G, \qquad \text{for } j = 1, \tag{23}$$

Equation (21) can be rewritten as

$$\sum_{j=1}^{J} \Delta n\, G_j\,(t_{d_j} + \lambda^{-1}) \leq \alpha\, V^{\text{crit}}, \tag{24}$$

with important property,

$$G_j \leq G. \tag{25}$$

Because of the above constraint, the approach is termed a reduced gradient bubble model (RGBM).

The terms $\Delta n\, G$ and $\Delta n\, G_j$ differ by the effective bubble elimination during the surface interval t_{j-1}. From (15) and (16), as seen, G requires long surface intervals to eliminate the excess bubbles, so that G_j must be reduced to compensate for the fact that large surface intervals are not available for bubble elimination over repetitive exposures. Having extracted G from the bounce and saturation data, we now turn to G_j for multi-exposures.

PHASE ASYMPTOTICS

The criterion (24) looks like a constraint on multiple bounce decompressions, with a repetitive growth rate, $\Delta n\, G_j$, less than the bounce growth rate, $\Delta n\, G$. A conservative set of repetitive gradients, G_j, satisfying the phase integral constraint, can be generated for repetitive activity, provided the bubble growth, regeneration and deeper excitation are reduced through the bubble fractions ξ, relating G_j and G

$$G_j = \xi_j\, G, \tag{26}$$

with ξ_j an *exposure* bubble fraction satisfying (25),

$$0 \leq \xi_j \leq 1, \tag{27}$$

so that the inflation rate is reduced, as needed,

$$\Delta n\, G_j \leq \Delta n\, G. \tag{28}$$

This reduction in G imparts a correspondingly shorter non-stop exposure limit, a *penalty* in effect, decreasing with ξ, obviously. Knowing the repetitive profiles ahead of time, we could iterate (24) over time, until a worthy set of G_j is obtained, satisfying all constraints, and that would be an optimal set. In an unplanned (free style) activity we cannot perform this exercise, so we must then conservatively estimate ξ ahead of time, based on the previous exposure history, surface intervals, non-stop limits and permissible tensions for bounce exposures.

As the surface time intervals decrease, the appropriate ξ_j should get smaller, and the staging approaches saturation limits as $J \to \infty$. As the surface time intervals increase, ξ_j should get larger, and the staging approaches bounce limits as $t_j \to \infty$. In between, the behavior depends on the total elapsed time, total surface interval, tissue compartment and profile.

In a bubble model, three free phase buildup factors need consideration: excitation on deeper-than-previous exposure, repetitive bubble inflation rate and micronuclei regeneration. Each suggests a multiplicative factor, η, to be applied to the permissible bounce gradients. Their application downscales the critical gradients, thereby reducing the driving term for free phase inflation the according to (21).

EXPOSURE FRACTIONS

Permitting regeneration [21], we reduce bubble excesses in time through $r(t)$ and $\Delta n(t)$, in writing

$$\Delta n(t) = N\beta r_0 \left(1 - \frac{r(t)}{r_0}\right) = \Delta n \ \exp\ (-\omega t), \tag{29}$$

using (8). The reduction factor, accounting for creation of new stabilized microbubbles, η_j^{regen}, is taken to be the ratio of the present excess, $\Delta n(t_j^{\text{cum}})$, over the initial excess, Δn,

$$\eta_j^{\text{regen}} = \frac{\Delta n(t_{j-1}^{\text{cum}})}{\Delta n} = \exp\ (-\omega\, t_{j-1}^{\text{cum}}), \qquad t_{j-1}^{\text{cum}} = \sum_{i=1}^{j-1} t_i, \tag{30}$$

with t_{j-1}^{cum}, the cumulative surface interval time. Since ω^{-1} is on the order of days, η_j^{regen} affects multi-day activities. The penalty for consecutive multi-day decompressions increases with frequency.

Successively deeper exposures excite additional micronuclei on each excursion. While this is not a good procedure even within a single decompression, it is well known to be hazardous in repetitive exposures. Deeper-than-previous exposures might excite new pools of smaller micronuclei into growth, occurring on top of the growth of larger micronuclei from previous exposures. If the phase elimination between exposures is not efficient, and earlier bubbles are approaching the critical number and size, the next deeper-than-previous exposure could excite enough additional bubbles to exceed V^{crit}. Diving within the crush limits of the first decompression is always prudent. To treat the ill-advised case of deeper-than-previous consecutive exposures, an excitation reduction factor, η_j^{excite}, is defined to be the minimum value of the ratio of the permissible bubble excesses on consecutive exposures to depth d,

$$\eta_j^{\text{excite}} = \frac{(\Delta n)_{\max}}{(\Delta n)_j} = \frac{(r\,d)_{\max}}{(r\,d)_j}, \tag{31}$$

with $(\Delta n)_{\max}$ evaluated at the deepest depth over segments, and $(\Delta n)_j$ equal to $(\Delta n)_{\max}$ until such a time when a greater depth is reached. The penalty for repetitive exposure, deeper than previous increases with the relative depth difference between the exposures.

The bounce gradients, G, assume long surface intervals for the elimination of excess bubbles, $\Delta n\, G(t_d + \lambda^{-1})$. Repetitive exposures do not allow that elimination to go to completion. Accordingly, repetitive gradients could be reduce to compensate for shorter periods of bubble elimination by a reduction factor, η_j^{phase}, linked to the radial expansion rate, $\dot{r}$,

$$\dot{r} = \frac{1}{r}\frac{DS}{C}(p - P - G^{\text{bub}}), \tag{32}$$

with p, the instantaneous tissue tension; P, the ambient pressure; G^{bub}, bubble surface tension pressure; and D, C and S, the tissue diffusivity, effective phase concentration and solubility. Throughout the course of any decompression, it would be possible, but tedious, to track $\dot{r}$. Making the assumption, then, that $\dot{r}$ decays exponentially over the characteristic surface time, χ^{-1} (see [7]), we write

$$\dot{r}(t_{j-1}) = \frac{1}{r}\frac{DS}{C}\,(G - G^{\text{bub}})\ \exp\ (-\chi\, t_{j-1}), \tag{33}$$

with t_{j-1}, the surface interval time. The gradient reduction factor, η_j^{phase}, is then taken to be the difference between the maximum and present radial rates, normalized to the maximum rate,

$$\eta_j^{\text{phase}} = 1 - \frac{\dot{r}(t_{j-1})}{(\dot{r})_{\max}} = 1 - \left(1 - \frac{G^{\text{bub}}}{G}\right) \exp\ (-\chi\, t_{j-1}), \qquad (\dot{r})_{\max} = \frac{1}{r}\frac{DS}{C}\,G. \tag{34}$$

The repetitive factor restricts multi-exposures over time intervals of hours, with χ^{-1} on the order of an hour. Early upon surfacing, the growth rate is large, the reduction factor small and, therefore, the penalty large, approaching G^{bub}/G_0 as the fractional multiplier.

Putting all of the above together, an exposure fraction ξ_j is defined at the start of each segment and deepest point of the exposure,

$$\xi_j = \eta_j^{regen}\,\eta_j^{phase}\,\eta_j^{excite}\,, \tag{35}$$

with the surface and cumulative surface intervals appropriate to the preceding segment. Since η_j are bounded by zero and one, ξ_j are similarly bounded by zero and one. Consistently with recent workshops and flying-after-diving recommendations, the terms in (35) might relax to one, following any 48 hour surface interval of non-diving. The tissue tensions and bubble excesses would tend to equilibrate with the ambient pressure on those time scales. At any rate, all η link to the bubbles or nuclei directly, as well as critical tensions.

PARAMETER SPACE AND CONSTANTS

The bubble growth factors, ξ, effectively penalize repetitive activity over short time spans, deeper-than-previous and continuous multi-day activity. Long surface intervals and breaks in multi-day activity reduce the penalty and restore the bounce gradients drawn in Figure 1. Obviously, this approach is not limited to the data employed herein. The ξ can be employed to any set of critical parameters.

For illustration, the repetitive, multi-day and excitation factors, η^{phase}, η^{regen} and η^{excite}, are drawn for representative choices of χ, G^{bub}, r_0 and ω. Figure 2 depicts η^{phase} in 40 min surface intervals for $\chi^{-1} = 40$ min and $G^{bub} = 8.3$ fsw. The multi-day factors, η^{regen}, are drawn for 14 days of diving in Figure 3. The excitation factors, η^{excite}, are depicted for $R_0 = 0.8$ microns at sea level in Figure 4. A direct (non-stop) ascent to the surface is assumed here for simplicity.

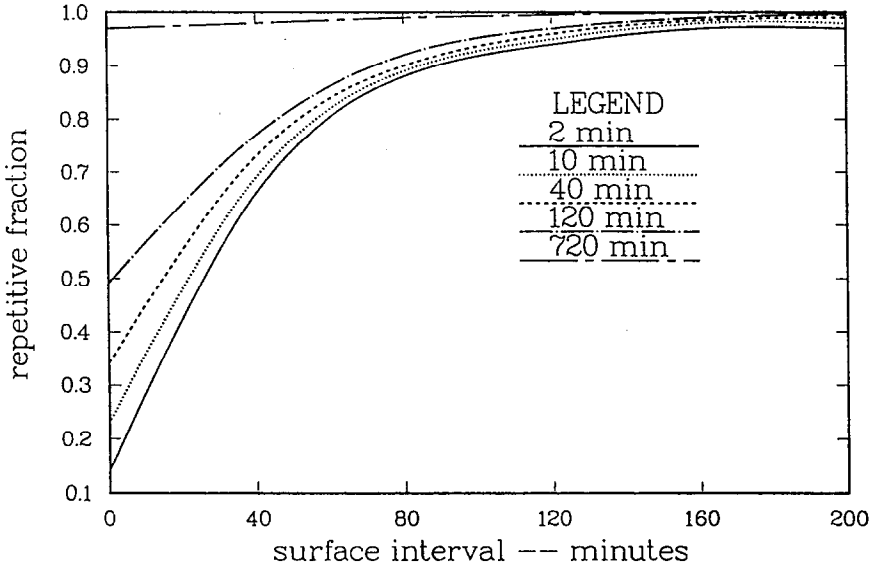

Figure 2. Repetitive reduction factors.

Clearly, the repetitive factors, η^{phase}, relax to one after about 2 hours, while the multi-day factors, η^{regen}, continue to decrease with the increasing repetitive activity, though at very slow rate. Obviously, increases in χ^{-1} and ω^{-1} will tend to decrease η^{phase} and increase η^{regen}. Figure 2 plots η^{phase} as a function of the surface interval in minutes for the 2, 10, 40, 120 and 720 min tissue compartments, while Figure 3 depicts η^{regen} as a function of the cumulative exposure in days for $\omega^{-1} = 7, 14$ and 21 days. The repetitive fractions, η^{phase}, are bounded by G^{bub}/G_0 at zero surface interval, obviously restricting the back to back repetitive activity considerably. The multi-day fractions approach zero as multi-day activities increase continuously beyond 2 weeks.

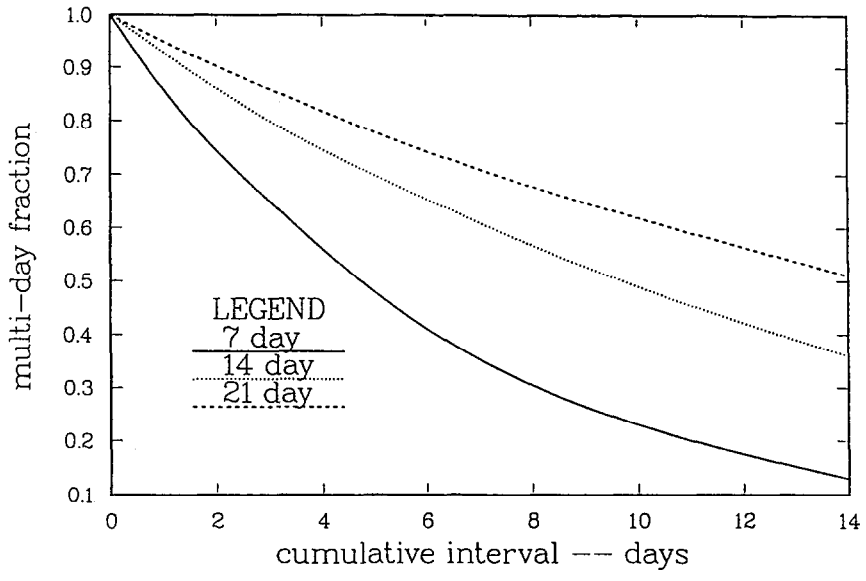

Figure 3. Multi-day reduction factors.

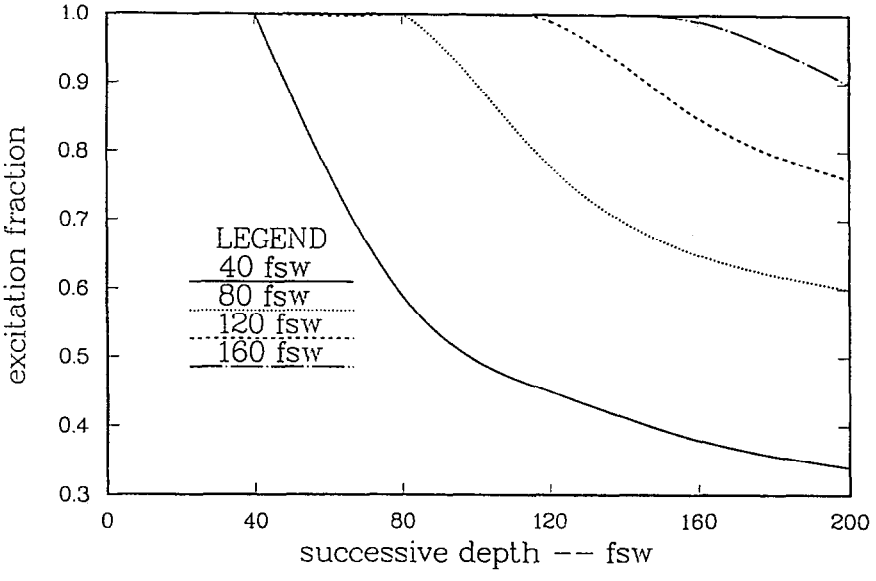

Figure 4. Excitation reduction factors.

The excitation factors, η^{excite}, are drawn in Figure 4 for exposures in the range 40–200 fsw. Clearly, deeper-than-previous excursions incur the greatest reductions in permissible gradients (smallest η^{excite}) as the depth of the exposure exceeds the previous maximum depth. Figure 4 depicts η^{excite} for various combinations of depths, using 40, 80, 120, 160 and 200 fsw as the first dive depth, d_{max}.

DIVING APPLICATION

As an application of the model, consider two repetitive dives a day, 120 fsw for 10 min separated by a 2 hour surface interval, over three consecutive days. This profile, extended to three repetitive dives a day, has produced bends in three out of four cases on the first day [27], so it is interesting. Products of η, from Figure 2 through 4, form ξ, as detailed. Employing an G^{bub} equal 8.3 fsw, slightly less than (7), taking $\omega^{-1} = 14$ days and $\chi^{-1} = 40$ min, we can compute ξ on each segment, and then compute the non-stop limits. The model reduces the permissible gradients in each tissue compartment, on each segment of the six dives, according to Table 1, which lists ξ at the start of each repetitive and multi-day segment. A systematic reduction is seen. The

corresponding critical tension can be computed from (4) and (6),

$$M = \xi G + P, \tag{36}$$

with quantities depicted in Figures 1 through 4. Such critical tensions are easily employed in Haldane algorithms, with non-stop parameterization, conservative already in itself. For a repetitive application, $0 \leq \xi \leq 1$, the corresponding critical tensions are even more conservative.

The reduction in gradients approach 20% in the fast compartments and 15% in the slower ones, on the last dive. On the first day, reductions in the fast compartments are near 5% on the second dive, and near 10% on the second dive of the second day. Smaller reductions, by a few percent, are seen in the slow compartments. The exposures in the 120 fsw range are controlled by the 10 min compartment, with 11 min the non-stop limit on the first dive ($\xi = 1$). On the sixth dive, the second dive of the third day ($\xi = .82$), the non-stop time limit drops to 7 min. On dives 2 through 5, the non-stop time limits obviously decrease monotonically within those same limits. The heavy multi-day, repetitive diving is obviously penalized the most in this approach. If deeper-than-previous exposures are attempted, additional restrictions are also imposed.

SUMMARY

Repetitive, deeper-than-previous, multi-day and multi-level decompression present problems for the Haldane model, which might be lessened in impact by a systematic reduction in the critical gradients, or tensions, consistent with bubble mechanics and the phase volume limit. The reductions are based on possible excitation and regeneration of micronuclei and bubble inflation rates and not on dissolved gas buildup *per se*. A model, called the reduced gradient bubble model, RGBM for short, has been described and applied to a marginal multi-day profile, illustrating systematic reductions in gradients, and hence non-stop time limits, across individual segments. Six consistent parameters codify the model, with five of them the original VPM parameters and the sixth appropriate to the RGBM, under meter study and development. Certainly the fractions, ξ, can be freed from any model connection, indeed, fitted to repetitive diving data. That avenue is also being pursued, mainly the correlations between data and Equations (30) through (35). Right now, there is paucity of multi-exposure data, but that should change in time.

REFERENCES

1. A.E. Boycott, G.C.C. Damant and J.S. Haldane, The prevention of compressed-air illness, *J. Hyg.* **8**, 342–443 (1908).
2. A.A. Buhlmann, *Decompression/Decompression Sickness*, Springer-Verlag, Berlin, (1984).
3. R.D. Workman, Calculation of decompression schedules for nitrogen-oxigen and helium-oxigen dives, USN Experimental Diving Unit Research Report, NEDU 6-65, Washington, D.C., (1965).
4. M.P. Spencer, Decompression limits for compressed air determined by ultrasonically detected blood bubbles, *J. Appl. Physiol.* **40**, 229–235 (1976).
5. H.R. Schreiner and R.W. Hamilton, Validation of decompression tables, Undersea and Hyperbaric Medical Society Publication, Bethesda, (1987).
6. A.R. Behnke, The application of measurements of nitrogen elimination to the problem of decompressing divers, *USN Med. Bull.* **35**, 219–240 (1937).
7. T.D. Kunkle and E.L. Beckman, Bubble dissolution physics and the treatment of decompression sickness, *Med. Phys.* **10**, 184–190 (1983).
8. E.D. Thalmann, Phase II testing of decompression algorithms for use in the US Navy underwater decompression computer, USN Experimental Diving Unit Report, NEDU 1-84, Panama City, (1984).
9. E.D. Thalmann, Air-N_2O_2 decompression computer development, US Navy Experimental Diving Unit Report, NEDU 8-85, Panama City, (1986).
10. F.P. Farm, E.M. Hayashi and E.L. Beckman, Diving and decompression sickness treatment practices among Hawaii's diving fishermen, University of Hawaii Sea Grant Report UNIHI-SEAGRANT-TP-86-01, Honolulu, (1986).
11. M.A. Lang and R.W. Hamilton, Proceedings of the American Academy of Underwater Sciences Dive Computer Workshop, University of Southern California Sea Grant Publication, USCSG-TR–01–89, Los Angeles, (1989).
12. A.M. Lang and G.H. Egstrom, *Proceedings of the American Academy of Underwater Sciences Biomechanics of Safe Ascent Workshop*, Diving Safety Publication AAUSDSP-BSA-01-90, Costa Mesa, (1990).
13. R.D. Vann, J. Dovenbarger, C. Wachholz and P.B. Bennett, Decompression sickness in dive computer and table use, *DAN Newsletter*, 3–6 (1989).

14. D.N. Walder, Adaptation to decompression sickness in Caisson work, *Biometeor.* **11**, 350–359 (1968).
15. A.A. Pilmanis, Intravenous gas emboli in man after compressed air ocean diving, Office of Naval Research Contract Report, N00014-67-A-0269-0026, Washington, D.C., (1976).
16. B.A. Hills, *Decompression Sickness*, John Wiley and Sons Inc., New York, (1977).
17. H.V. Hempleman, Further basic facts on decompression sickness, Investigation into the Decompression Tables, Medical Research Council Report, UPS 168, London, (1957).
18. D.I. Yount and R.H. Strauss, Bubble formation in gelatin: A model for decompression sickness, *J. Appl. Phys.* **47**, 5081–5089 (1976).
19. T.R. Hennessy and H.V. Hempleman, An examination of the critical released gas concept in decompression sickness, *Proc. Roy. Soc. London B* **197**, 299–313 (1977).
20. B.R. Wienke, Tissue gas exchange models and decompression computations: A review, *Undersea Biomed. Res.* **16**, 53–89 (1989).
21. D.E. Yount and D.C. Hoffman, On the use of a bubble formation model to calculate diving tables, *Aviat. Space Environ. Med.* **57**, 149–156 (1986).
22. D.E. Yount, On the evolution, generation and regeneration of gas cavitation nuclei, *J. Acoust. Soc. Am.* **71**, 1473–1481 (1982).
23. D.E. Yount, Skins of varying permeability: A stabilization mechanism for gas cavitation nuclei, *J. Acoust. Soc. Am.* **65**, 1431–1439 (1979).
24. D.E. Yount, C.M. Yeung and F.W. Ingle, Determination of the radii of gas cavitation nuclei by filtering gelatin, *J. Acoust. Soc. Am.* **65**, 1440–1450 (1979).
25. D.E. Yount, E.W. Gillary and D.C. Hoffman, A microscopic investigation of bubble formation nuclei, *J. Acoust. Soc. Am.* **76**, 1511–1521 (1984).
26. P.J. Sheffield, Flying after diving, Undersea and Hyperbaric Medical Society Publication 77 (FLYDIV), Bethesda, (1989).
27. D.R. Leitch and E.E.P. Barnard, Observation on no-stop and repetitive air and oxynitrogen diving, *Undersea Biomed. Res.* **9**, 113–129 (1982).